

Hydrogen and Fuel Cells Program
2015 Annual Merit Review and Peer Evaluation Meeting
Arlington, Virginia – June 8-11, 2015

Non-Precious Metal Fuel Cell Cathodes: Catalyst Development and Electrode Structure Design

Piotr Zelenay

***Los Alamos National Laboratory
Los Alamos, New Mexico 87545***

Project ID: FC107

Timeline

- **Project start date:** April 1, 2013
- **Project end date:** March 31, 2016

Budget

- **FY14 DOE funding:** \$1,275K
- **Planned FY15 funding:** \$1,275K
- **Total DOE project value:** \$3,999K
- **Cost share:** 20.1%

Barriers

- **A. Cost** (catalyst)
- **D. Activity** (catalyst; MEA)
- **B. Durability** (catalyst; MEA)
- **C. Power density** (MEA)

Partners – Principal Investigators

Carnegie Mellon University



– Shawn Litster

University of Rochester



– Michael Neidig

University of Waterloo



– Zhongwei Chen

Oak Ridge National Laboratory



– Karren More

IRD Fuel Cells



– Madeleine Odgaard

General Motors



– Joseph Ziegelbauer

Relevance: Objectives & Targets

Objectives:

Advance non-PGM cathode technology through the development of new materials and implementation of novel electrode concepts, together resulting in:

- (a) high ORR activity, viable for practical automotive systems
- (b) improved catalyst durability
- (c) high ionic/electronic conductivity within the catalyst layer
- (d) adequate oxygen mass transport and effective removal of the product water

Technical Targets (adjusted to follow current CWG recommendations):

Characteristic	Unit	2011 Status	Targets	
			2017	2020
Non-Pt catalyst activity per volume of supported catalyst	A / cm ³ @ 800 mV _{IR-free}	60 (measured at 0.8 V) 165 (extrapolated from >0.85 V)	300	300

- Catalyst activity in H₂/O₂ MEA at 0.044 A cm⁻² (80°C): ≥ 0.87 V (*iR*-free)
- Four-electron selectivity (RRDE): $\geq 99\%$ (H₂O₂ yield $\leq 1\%$)
- MEA maximum power density at 80°C: ≥ 1.0 W cm⁻²
- Performance loss at 0.80 A cm⁻² after 30,000 cycles in N₂: $\leq 40\%$

Approach: Details

Catalyst Activity

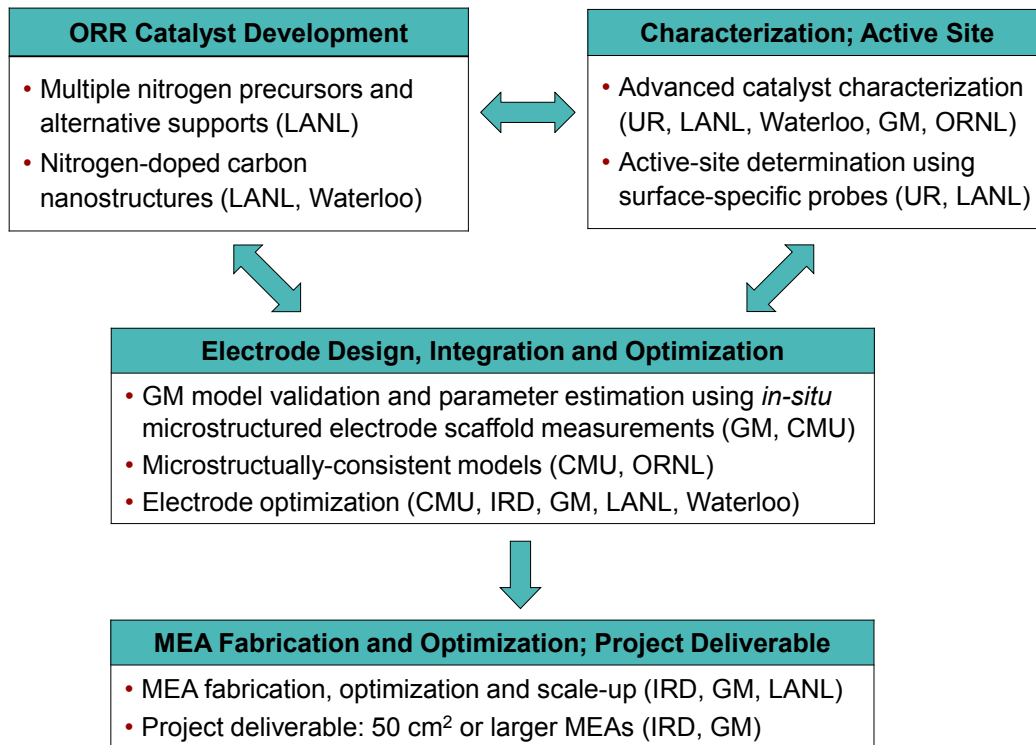
- Develop new syntheses to increase activity and active-site density
- Tune porosity to improve accessibility of ORR active sites
- Probe active sites to understand structure-activity relationships
- Explore synergies between multiple metal precursors

Durability

- Use durable non-carbon supports to mitigate corrosion
- Minimize and eliminate spectator species in Fe-based catalysts; explore catalysts synthesized using Fe-free precursors
- Improve durability by advanced cathode design (effective water management)

MEA Performance

- Image, model and optimize performance of non-PGM cathode structures



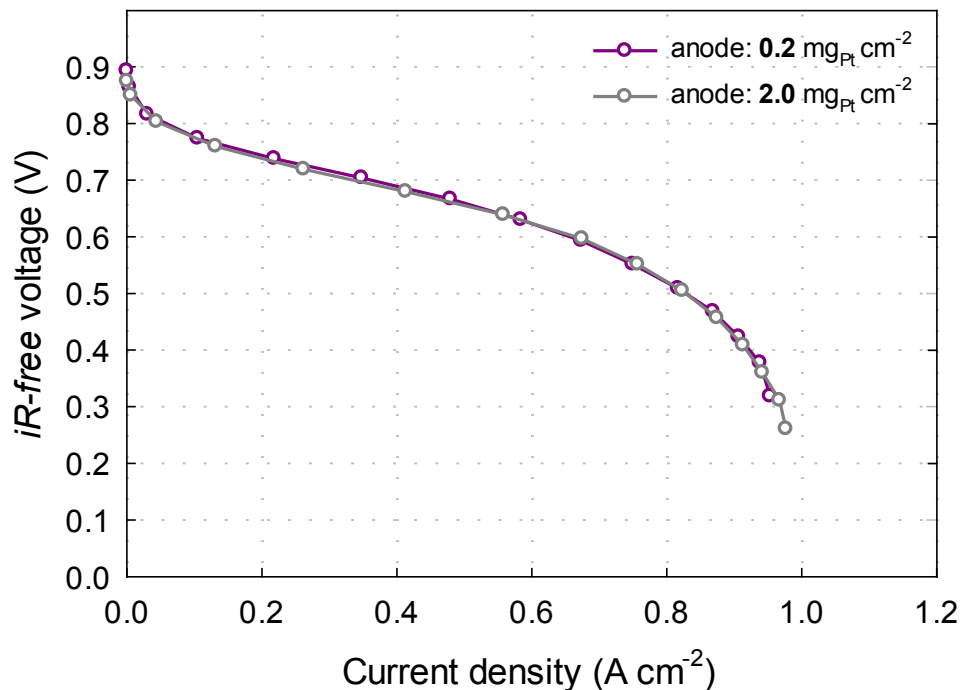
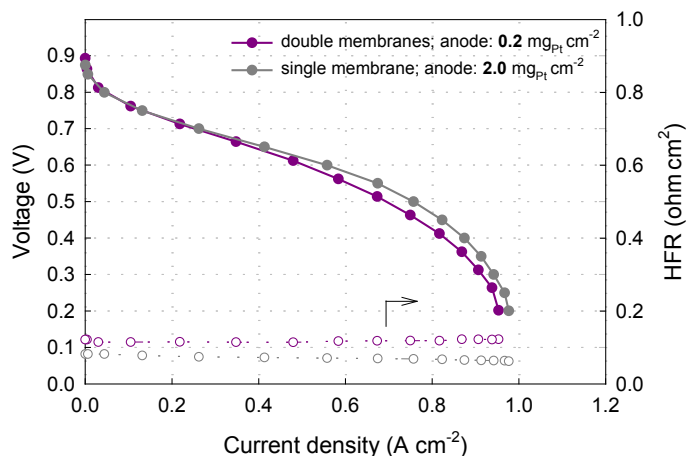
Approach: Project Milestones

Date	Quality Performance Measures and Milestone	Status	Comments
Dec 2014	Develop and validate a non-PGM cathode model that uses microstructurally-consistent agglomerate model with structural parameters from nano-XRT at CMU and electron microscopy at ORNL; perform validation against LANL single-cell testing and CMU's microstructured-electrode-scaffold measurements. QPM	Complete	Demonstrated performance validation against LANL single-cell testing and CMU's microstructured electrode-scaffold (MES) measurements, using a non-PGM cathode agglomerate model.
Mar 2015	Develop a preliminary model for PANI- and/or CM-derived ORR catalysts from surface-probe characterization data. QPM	Complete	Model developed based on NRVS and Mössbauer experiments involving PANI- and CM- catalysts; DFT used for data interpretation.
Jun 2015	Demonstrate $\geq 100 \text{ mA cm}^{-2}$ at 0.80 V (<i>iR</i> -corrected, air), $\eta > 95\%$, and 30,000-cycle performance loss of no more than 50 mV ($\Delta E_{1/2}$ and/or ΔV at 0.80 A cm^{-2}). Milestone	Pending	<i>Current status:</i> 90 mA cm⁻² at 0.80 V; $\eta > 97\%$; <i>ca. 30 mV</i> performance loss at $E_{1/2}$ after 30,000 cycles
Sep 2015	Scale-up MEA to at least 50 cm ² with selected non-PGM catalyst; demonstrate 0.80 V with at least 100 mA cm ⁻² (<i>iR</i> -corrected, air). QPM	Pending	Electrode structure optimization ongoing at IRD Fuel Cells and LANL; GM to be involved in testing
<p>Go/no-go decision for further development of metal-free catalysts based on nitrogen-doped nanostructures (demonstrate $E_{1/2} \geq 0.60 \text{ V}$ vs. RHE): no go (September 2014)</p>			

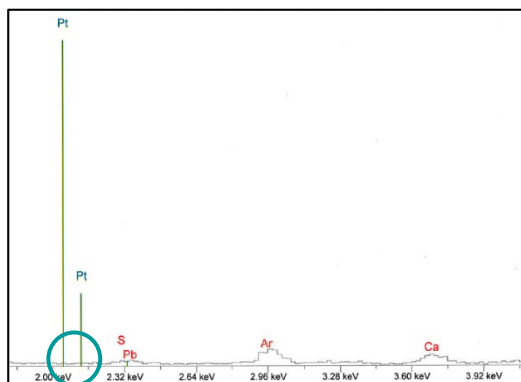
Response to 2014 Review Comments: Pt Crossover?

“Results clouded by exceptionally high anode Pt loadings (2 mg/cm²).” “[...] crossover of Pt needs to be excluded to affirm that this activity is not due to Pt crossed over from the anode.”

Anode: 2.0 or 0.2 mg_{Pt} cm⁻² Pt/C H₂, 200 sccm, 1.0 bar H₂ partial pressure; **Cathode:** ca. 4.0 mg cm⁻² air, 200 sccm (2.5 stoichiometry at 1.0 A cm⁻²), 1.0 bar air partial pressure; **Membrane:** single/double Nafion[®] 211; **Cell:** 80°C



Cathode XRF after Fuel Cell Testing



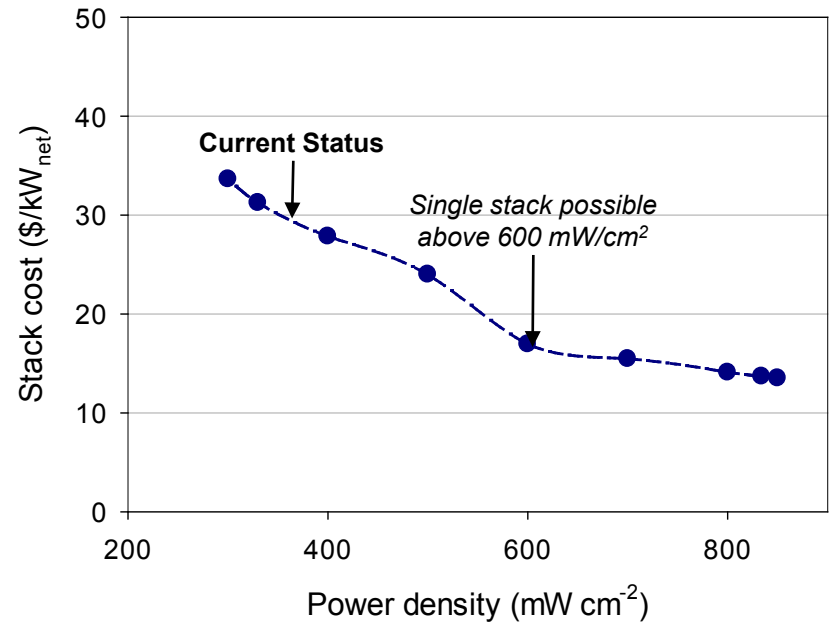
- As expected, fuel cell performance found to be independent of the anode Pt loading (2.0 vs. 0.2 mg_{Pt} cm⁻²)
- No Pt detected by XRF on the cathode electrode (in confirmation of earlier results); Pt crossover excluded

Response to 2014 Review Comments: Cost Analysis

“[...] cost projection must be studied [...]”

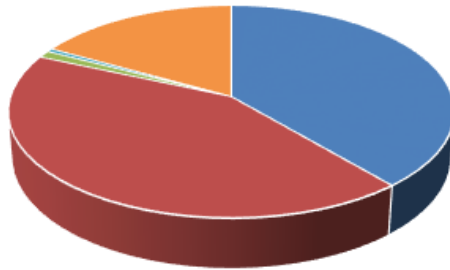
Catalyst Cost for 80 kW Stack (\$/kW)				
Production (systems/year)	1,000	10,000	100,000	500,000
\$/kW	0.62	0.43	0.37	0.35

Effect of MEA Power Density on Stack Cost (H₂-air; 1.5 bar total H₂ and air pressure)



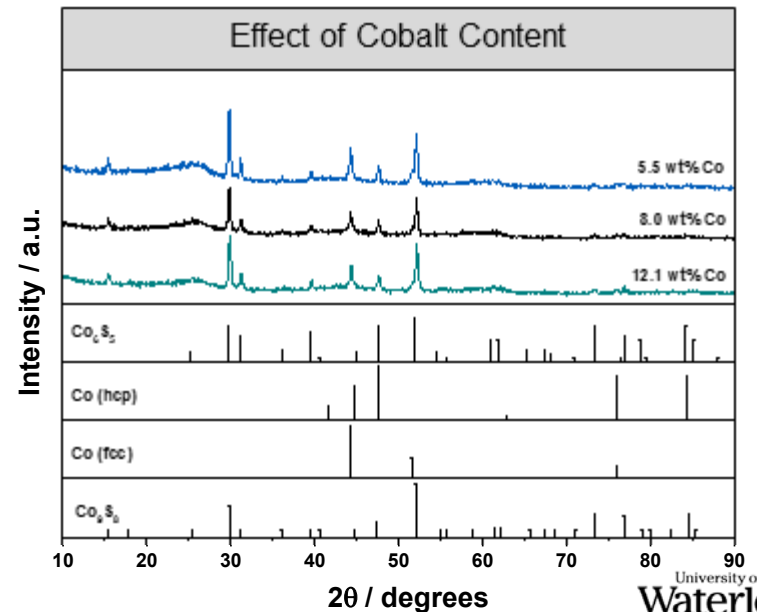
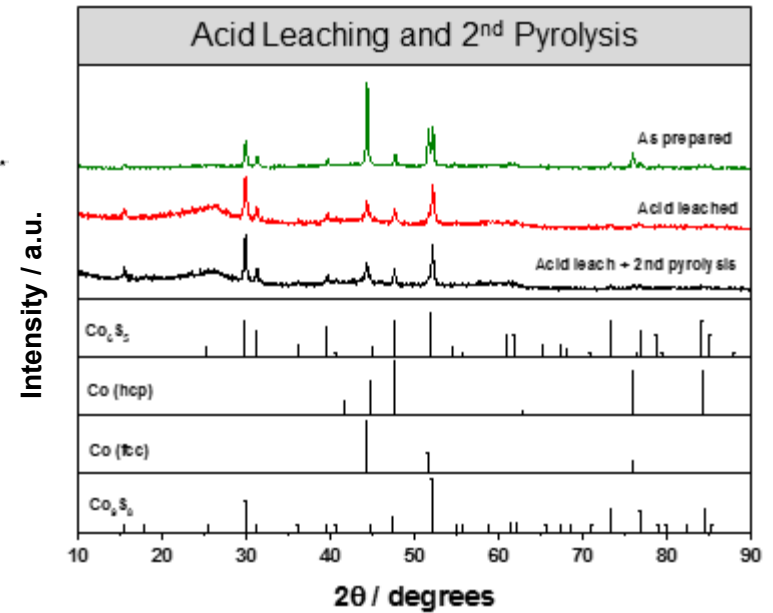
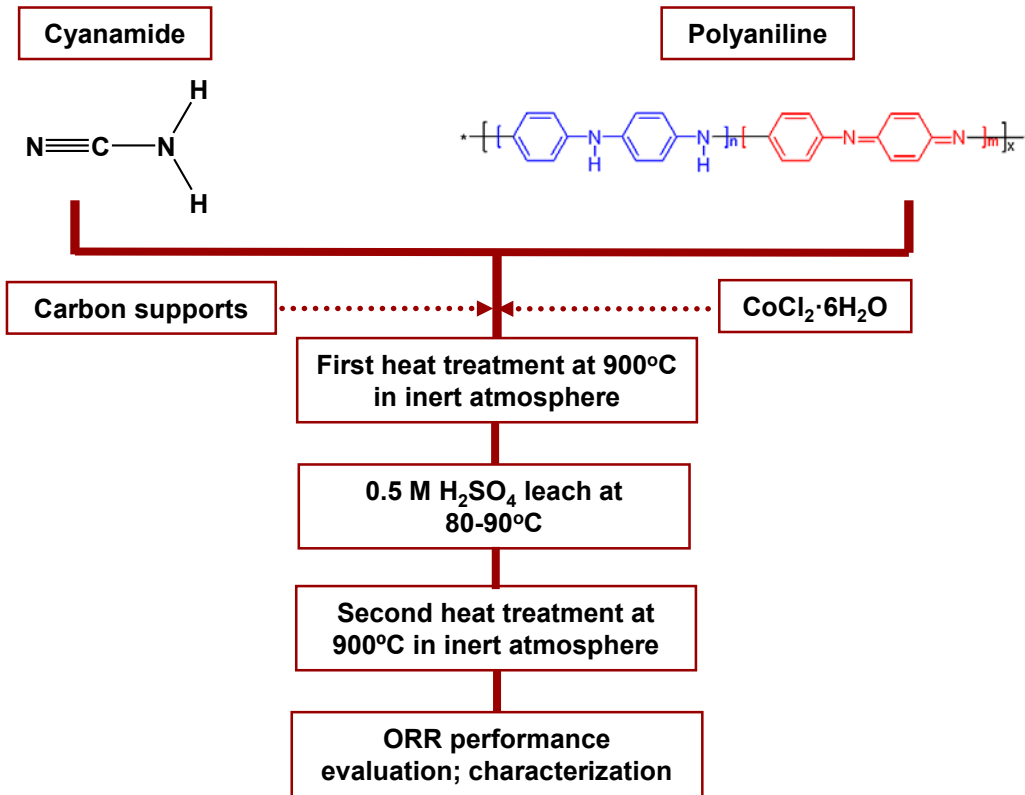
PANI-Fe-C Catalyst Manufacturing Cost Breakdown

- Carbon activation
- Catalyst reaction
- Drying
- Grinding
- Rotary kiln pyrolysis
- Acid leaching
- Oven pyrolysis



- **Highlight:** Preliminary analysis of PANI-Fe-C cost confirming major cost advantage of non-PGM ORR catalysts over state-of-the-art Pt-based catalysts by a factor of **ca. 550**
- Specific power density of non-PGM MEAs in need of improvement from the current level of **ca. 370 mW cm⁻²** in order for catalyst cost to make significant impact on the stack cost

Fe-free Catalyst: CM-PANI-Co-C

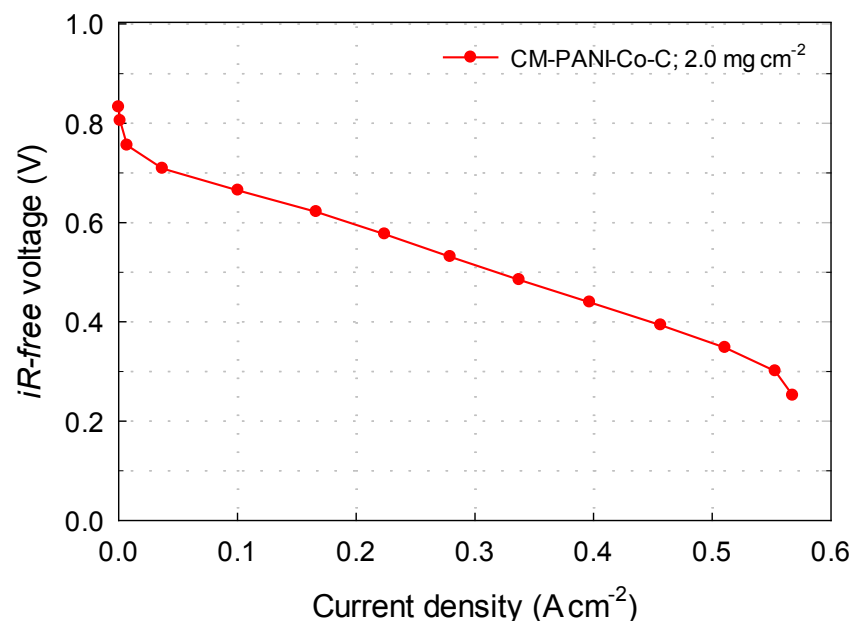
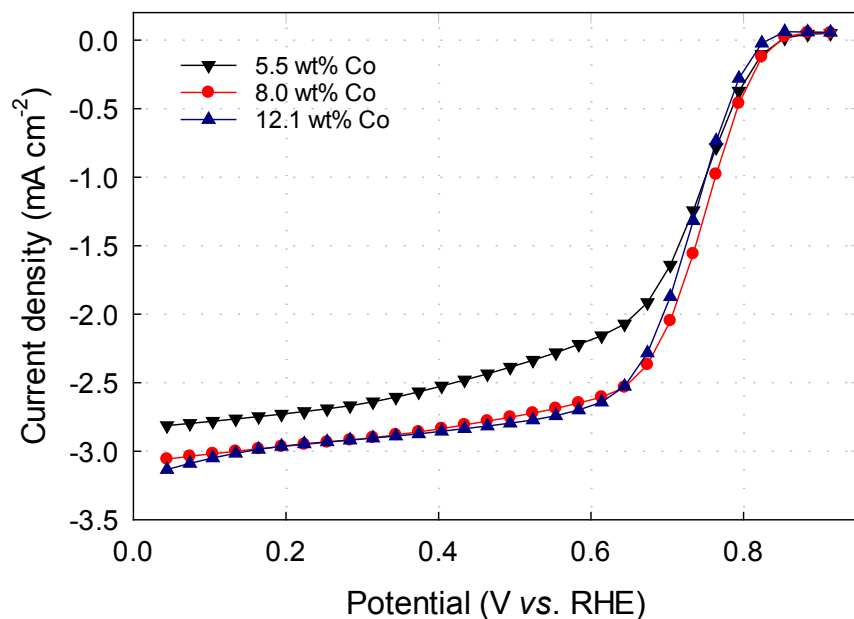


- Cobalt sulfides (Co₉S₈ and Co₆S₅) and metallic hcp and fcc Co observed in as-prepared samples
- Free-metallic fcc Co removed by acid leaching
- Co content having negligible effect on the phase speciation and structure

CM-PANI-Co-C: Effect of Co Content; MEA Performance

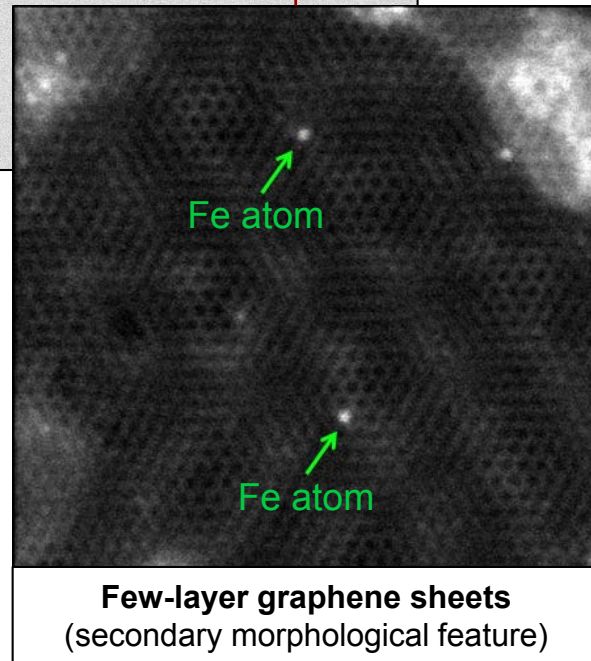
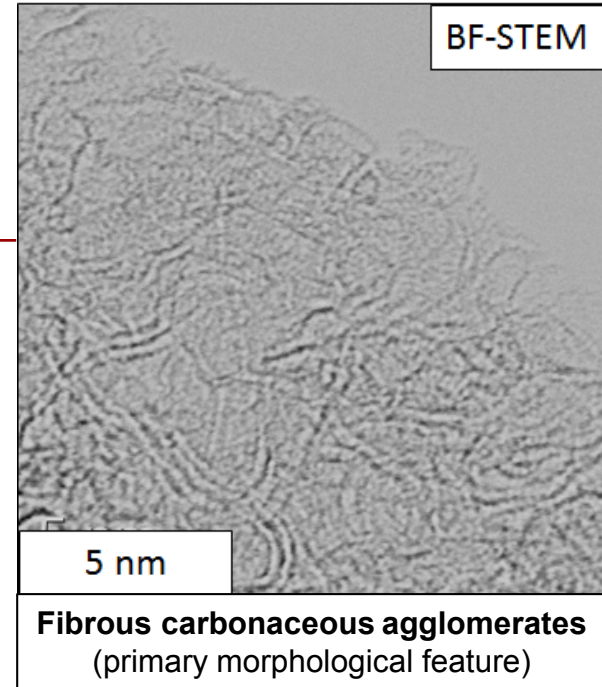
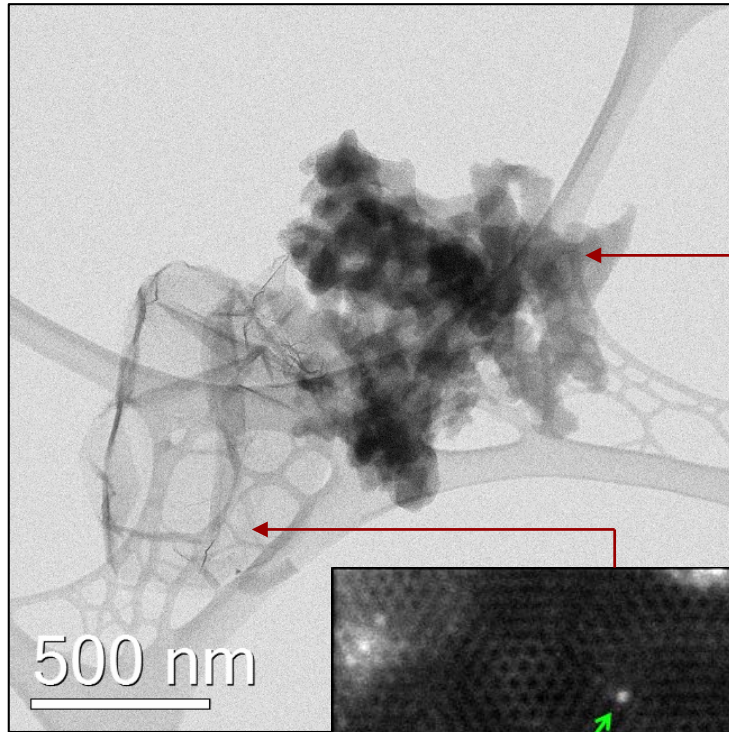
ORR: 0.6 mg cm⁻²; 0.5 M H₂SO₄; 900 rpm; 25°C; Hg/HgSO₄ (0.5 M H₂SO₄) reference electrode; graphite counter electrode; steady-state potential program: 30 mV steps, 30 s/step;

Anode: 0.2 mg_{Pt} cm⁻² Pt/C H₂, 200 sccm, 1.0 bar H₂ partial pressure; **Cathode:** 8.0 wt% Co catalyst air, 200 sccm, 1.0 bar air partial pressure; **Membrane:** double Nafion® 211; **Cell:** 80°C



- Highest RDE activity recorded with 8.0 wt.% Co catalyst; $E_{1/2}$ of 0.74 V reached
- **Highlight:** While trailing RDE and fuel cell performance of the best Fe-based catalysts, CM-PANI-Co-C found to show promising activity, warranting future research

CM-PANI-Fe-C Catalyst: Morphology

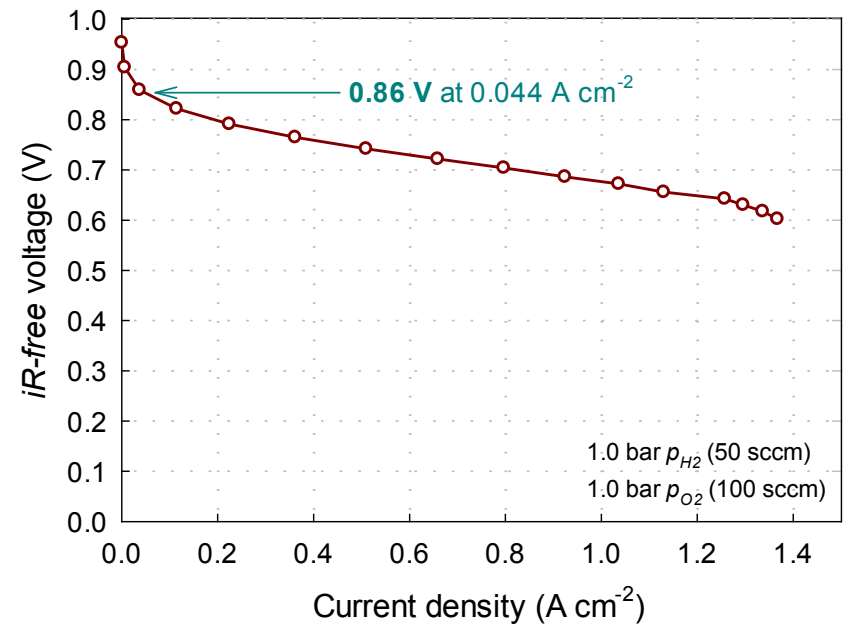
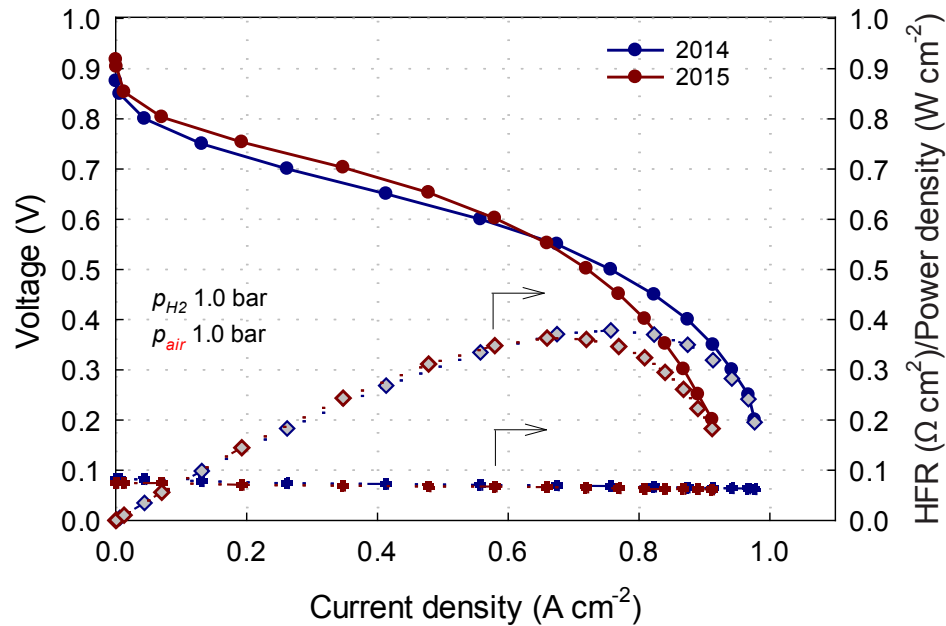


- CM-PANI-Fe-C catalyst consisting of fibrous carbonaceous agglomerates (randomly oriented, intertwined graphitic domains) and layered graphene sheets
- Graphene sheets associated with Fe/FeS particles, with a majority of Fe atoms dispersed on surfaces

CM-PANI-Fe-C: Progress in Catalytic Activity

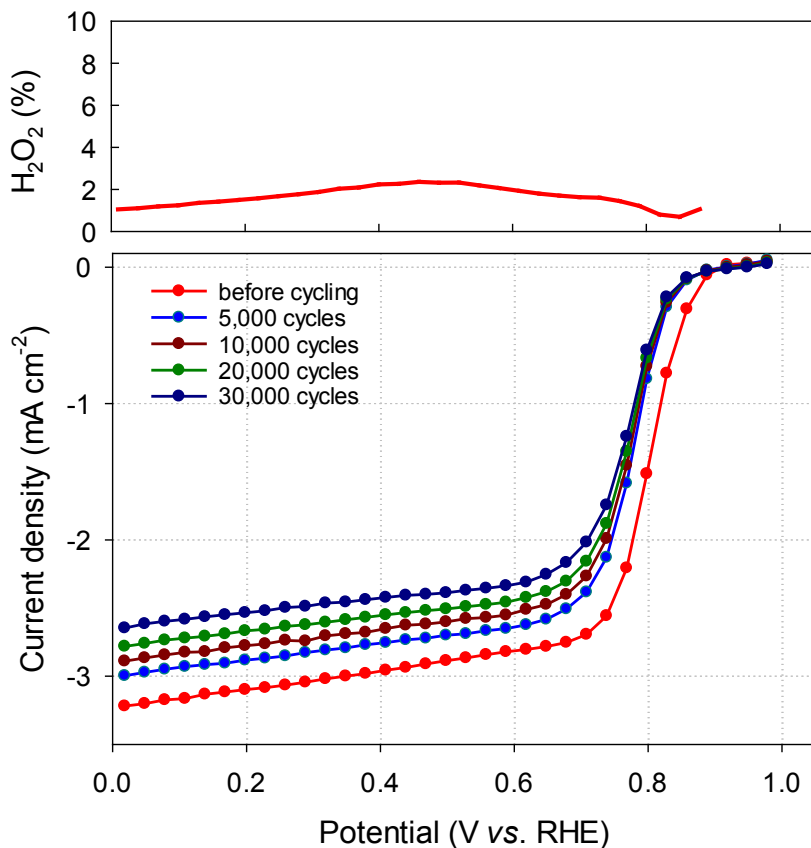
Anode: 2.0/0.2 mg_{Pt} cm⁻² Pt/C H₂, 200 sccm, 1.0 bar H₂ partial pressure;
Cathode: ca. 4.0 mg cm⁻² air, 200 sccm, 1.0 bar air partial pressure;
Membrane: Nafion®211; **Cell size:** 5 cm²

Anode: 0.2 mg_{Pt} cm⁻² Pt/C H₂, 50 sccm, 1.0 bar H₂ partial pressure;
Cathode: ca. 4.0 mg cm⁻² O₂, 100 sccm, 1.0 bar O₂ partial pressure; **Membrane:** Nafion®117; **Cell size:** 5 cm²

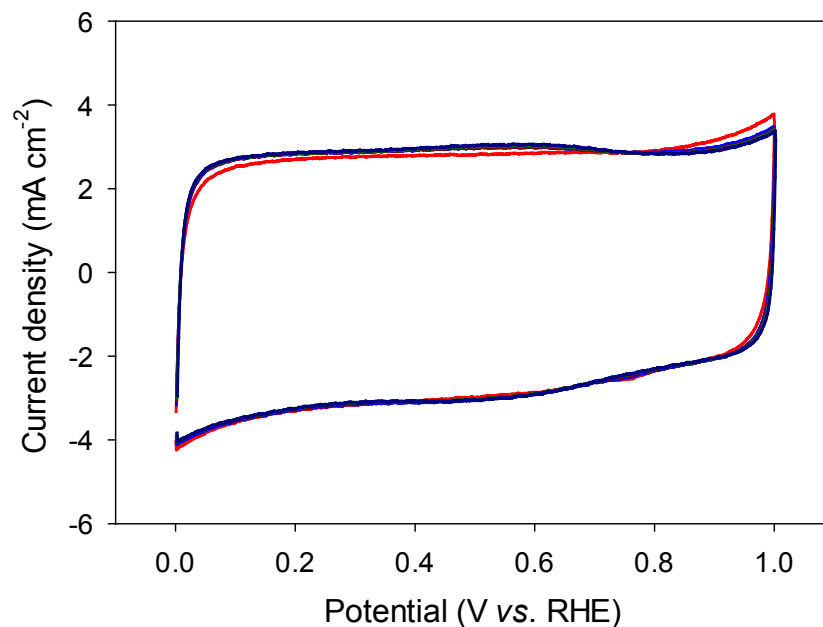


- Notable improvement in H₂-air fuel cell performance of CM-PANI-Fe-C catalyst
- **Highlight:** 0.044 A cm⁻² reached at **0.86 V** (*iR-free*) in H₂-O₂ fuel cell test (**0.01 V** away from the 2020 non-PGM activity target of 0.87 V)

CM-PANI-Fe-C Catalyst: H₂O₂ Yield and Cycling Durability



ORR: 0.5 M H₂SO₄; 900 rpm; 25°C; Hg/HgSO₄ (0.5 M H₂SO₄) reference electrode; graphite counter electrode; steady-state potential program: 30 mV steps, 30 s/step; **CV:** 0.5 M H₂SO₄; 0 rpm; 25°C; 20 mV/s; **Durability cycling:** 0.2 - 1.0 V; N₂ saturation; 200 mV/s

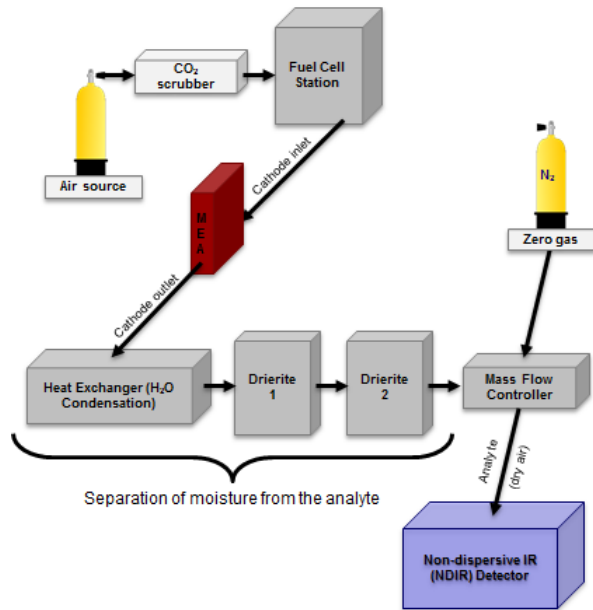


- **Highlight:** Potential loss at $E_{1/2}$ after 30,000 cycles between 0.2 and 1.0 V in N₂-saturated electrolyte: ca. **30 mV**
- H₂O₂ yield < **2%** in the entire ORR potential range

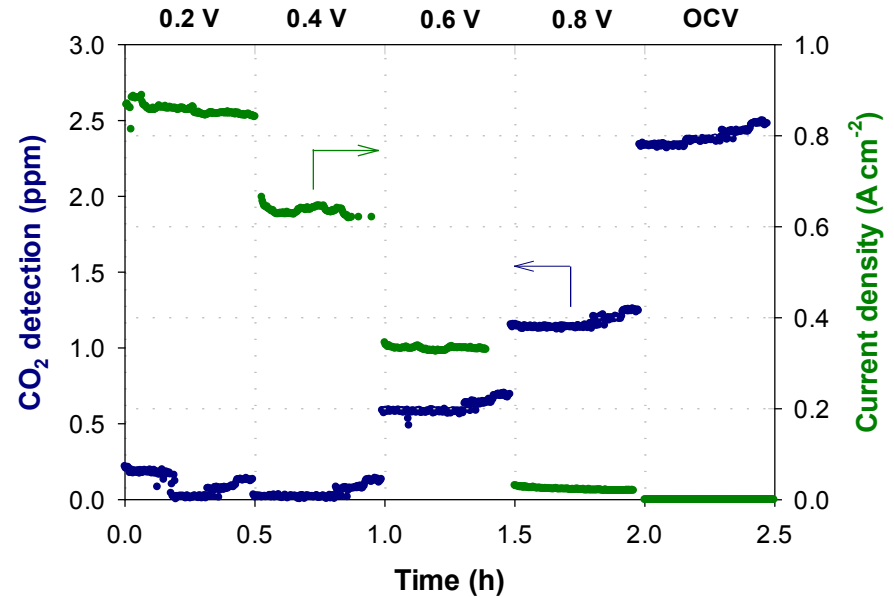
June 2015 durability and selectivity targets achieved and exceeded

In situ CO₂ Detection; TEM Analysis after Cycling Test

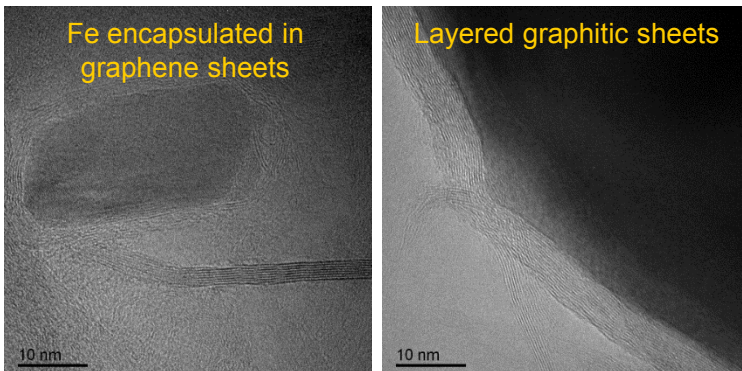
Schematic of CO₂ Detection Setup



Anode: 0.2 mg cm⁻² Pt; **Cathode:** 4.0 mg cm⁻² CM-PANI-Fe-C; **Membrane:** 211 Nafion®; **Cell:** 80°C; 100% RH, total pressure 1.5 bar; 400 sccm, 30 min/voltage step

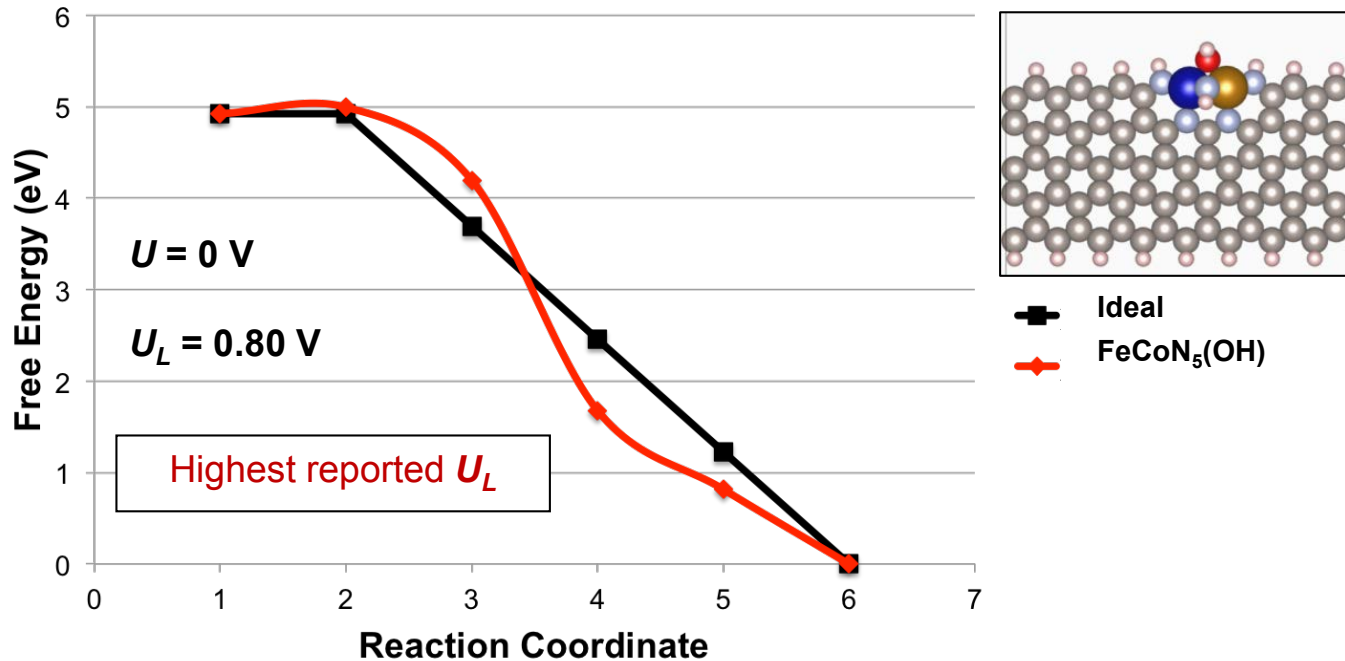


TEM of Catalyst Layer after 3,000 Cycles in Air



- **Highlight:** CO₂ detection setup designed, tested, and used for corrosion measurements
- Increased CO₂ generation observed at higher voltages (up to 5 ppm at OCV)
- Carbon morphology unaltered by corrosion testing; no loss in graphitic content, no evidence of carbon oxidation (TEM)
- No Fe detected in the membrane (important for ionomer durability)

Most Active Structure Based on Thermodynamic Limiting Potential



Calculation of thermodynamic limiting potential, U_L , with computational hydrogen electrode and DFT of ORR intermediate binding energies

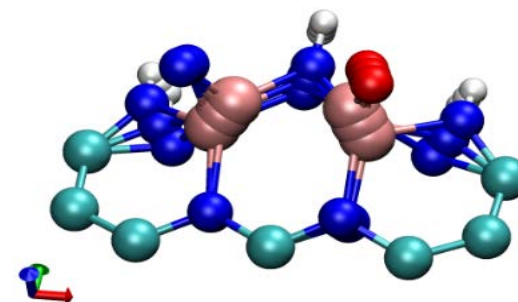
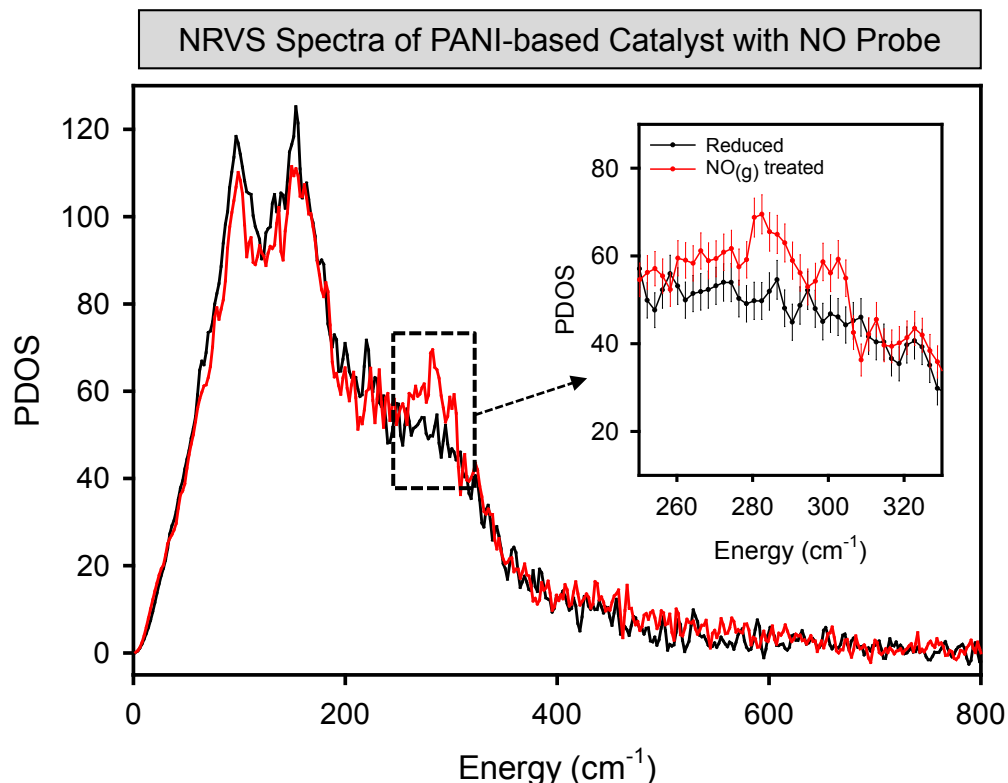
- U_L maximum at 1.23 V (higher \rightarrow more active)
- *OH ligand spontaneously formed in water-bearing environments, modifies site, improving predicted activity

$\text{Fe}_2\text{N}_5(\text{OH})$ $U_L = 0.72 \text{ V}$

$\text{FeCoN}_5(\text{OH})$ $U_L = 0.80 \text{ V}$

- **Highlight:** Most active reported structure to date based on thermodynamic stability arguments

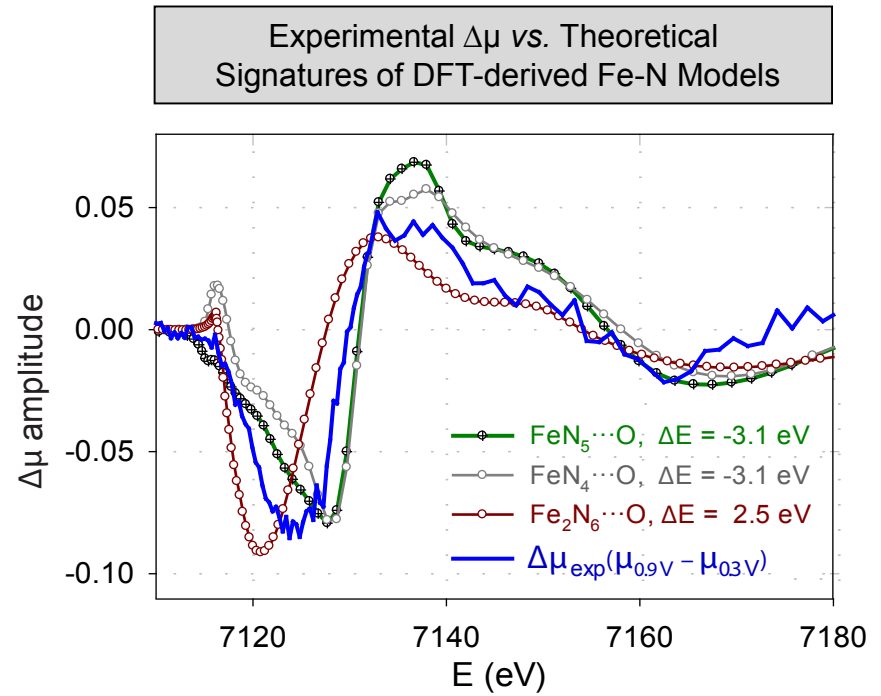
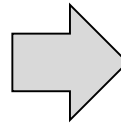
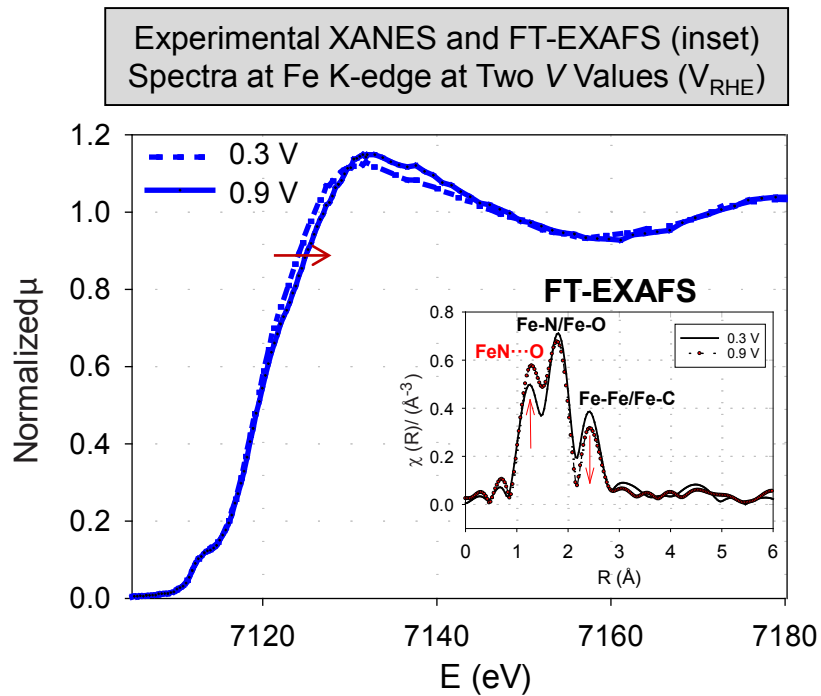
Mapping Atomic-Scale Active-Site Structures to Experimental Signatures



Fe₂N₅ model active site found to spontaneously dissociate O₂ when reduced and dissociate N₂ with small barrier → likely to also spontaneously cleave N-O bond

- Spectra with and without NO probe molecule: (i) major change at ~ 280-300 cm⁻¹ → Fe gas-phase accessible; NO interacting directly with Fe
- NRVS with NO probe molecule suggesting NO dissociation (Fe-N and Fe-O vibrations, shoulders ~ 200-400 cm⁻¹ vs. 600-700 cm⁻¹ expected for non-dissociated Fe-NO)
- DFT-calculated spectra of dissociated NO on Fe₂N₅ yielding vibrational modes at 260, 266, and 302 cm⁻¹ → consistent with experimentally observed vibrations
- **Highlight:** Fe₂N₅ active-site model predicting NO dissociation and NRVS peaks (**March 2015 QPM**)

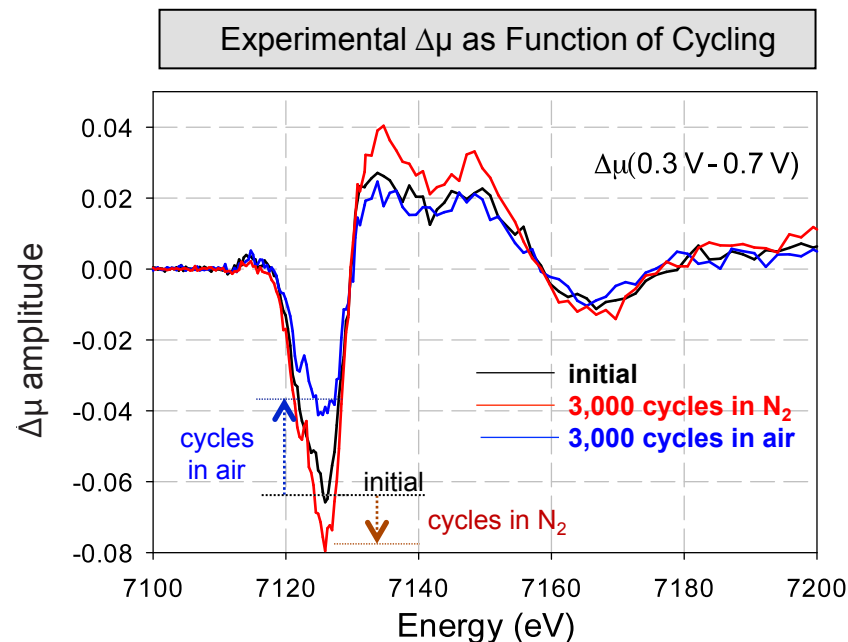
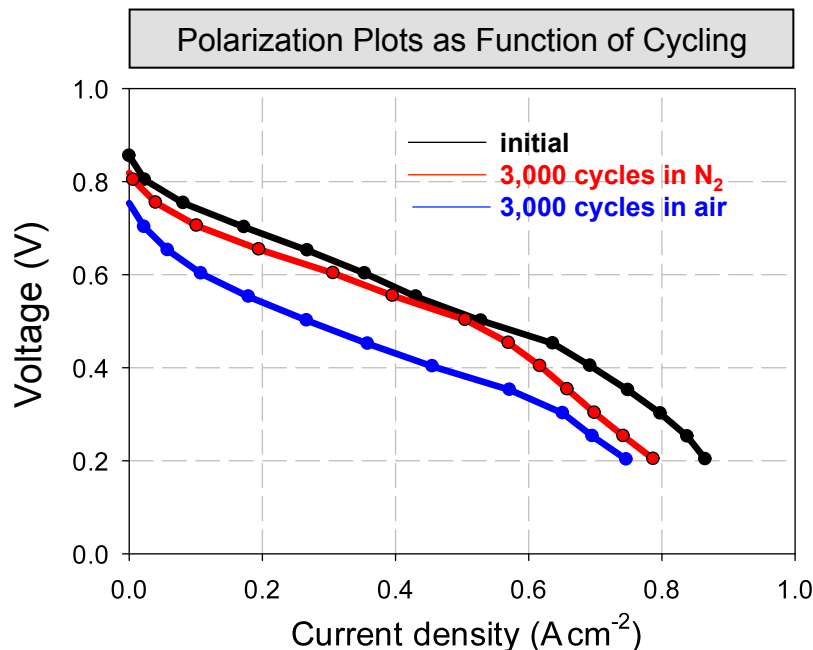
PANI-Fe-C Catalyst Study by XAS



- ~1 eV XANES shift suggesting Fe²⁺-to-Fe³⁺ transition
- Fe-N···O FT-EXAFS peak amplitude change indicative of a bond formation between Fe-N_x and O
- **Highlight:** Experimental $\Delta\mu$ in good agreement with theoretical DFT-derived structures, such as Fe₂N₆, FeN₄, and FeN₅ (pure or mixed)
- Ongoing DFT + FEFF calculations of Fe₂N₅OH (previously identified at LANL)

In situ XAS/ $\Delta\mu$ -XANES Study of CM-PANI-Fe-C Performance

Anode: 0.2 mg cm⁻² Pt; **Cathode:** 5 cm², CM-PANI-Fe-C catalyst, 4.0 mg cm⁻²; **Cell:** 80°C; 100% RH, total pressure: 2 bar
Membrane: Nafion® 211; **Cycling:** 3,000 cycles, H₂/N₂ and H₂/air; **XAS cell:** 80°C; 75% RH



$$\Delta\mu_{observed} = \frac{Fe_{Fe-N}}{Fe_{total}} \Delta\mu_{Fe-N}$$

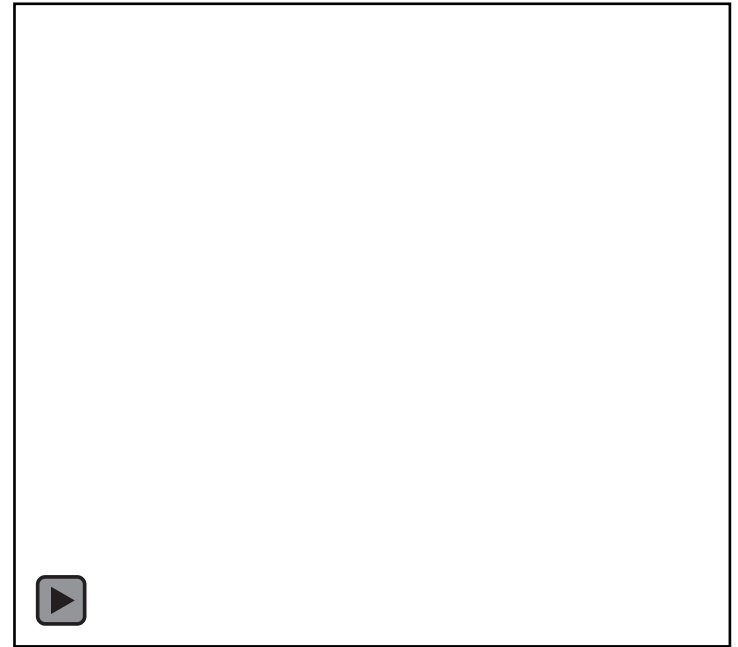
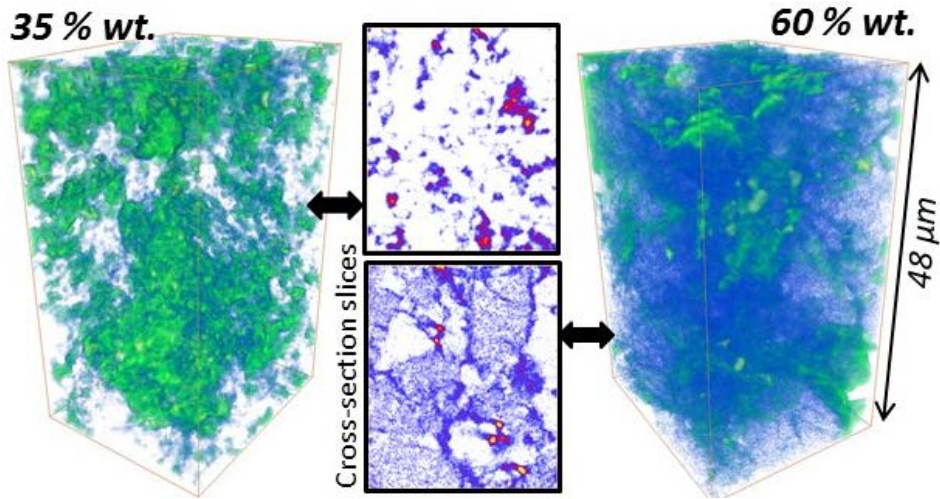
- Fe_{Fe-N} - Fe atoms contributing to $\Delta\mu$ signal
- Fe_{total} - total Fe atoms detected by XAS
- $\Delta\mu_{observed}$ - observed amplitude of $\Delta\mu$ signal
- $\Delta\mu_{Fe-N}$ - amplitude of $\Delta\mu$ assigned to Fe_{Fe-N}

- Very small change in performance after cycling in N₂: Fe-N_x centers intact (increase in $\Delta\mu$ caused by removal of spectator Fe species)
- Performance loss after cycling in air: Fe-N_x removed; $\Delta\mu$ amplitude decreased
- **Highlight:** Fe-N_x centers likely responsible for ORR activity

Soft X-ray experiments ongoing (collaboration with Stanford University)

Nano-XRT and 3D Nafion® Mapping

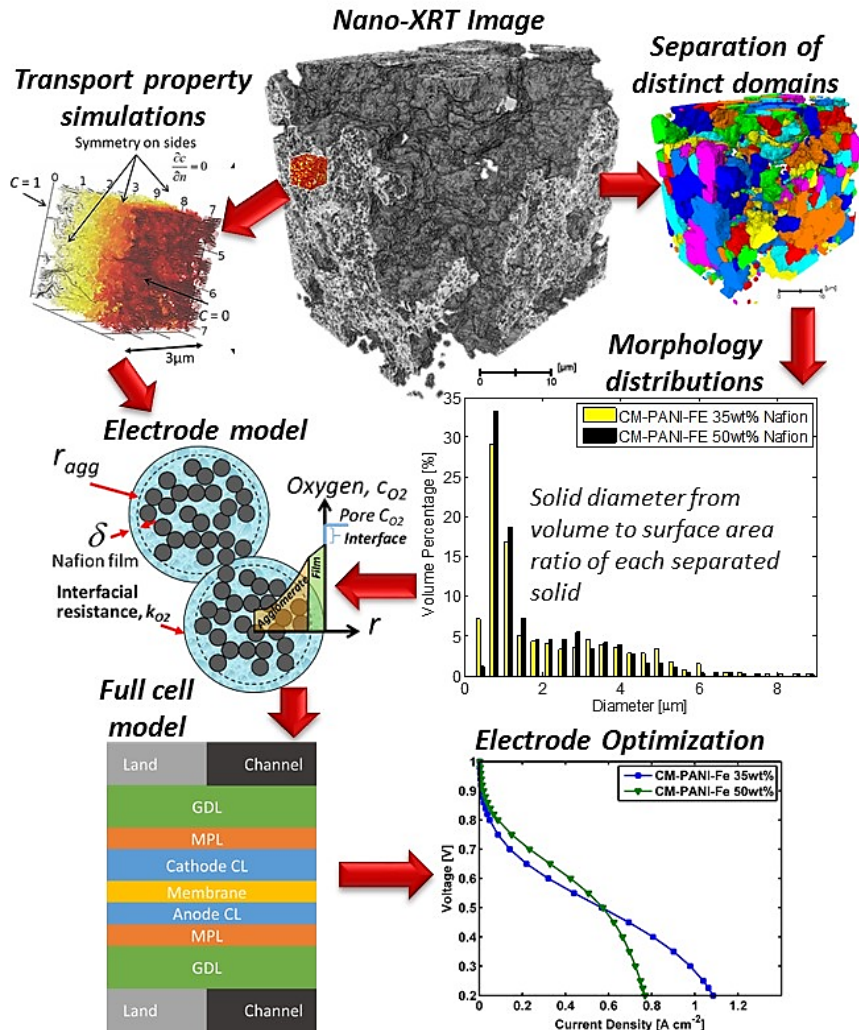
3D Nafion® Density Maps for Two Loadings



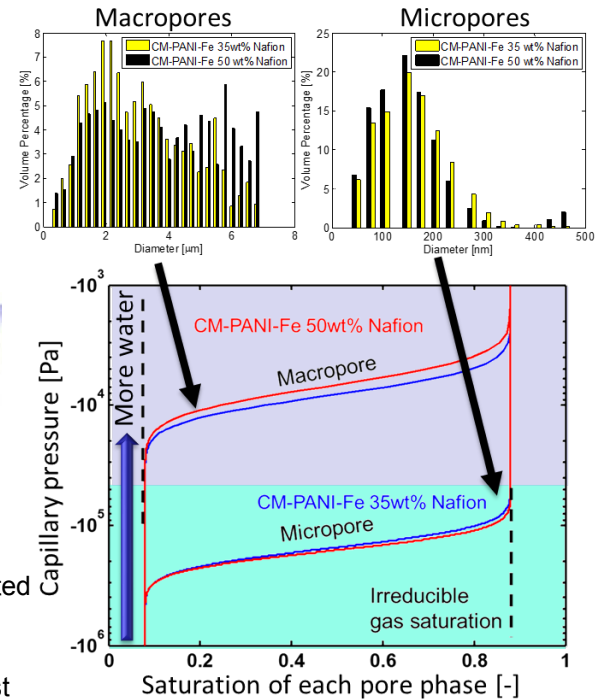
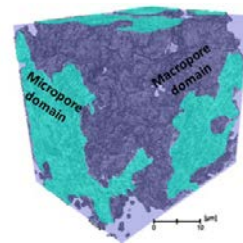
- Cs⁺ staining of Nafion® to separately map **catalyst** (Zernike phase contrast) and **Nafion®** (absorption contrast) at 50 nm resolution; average Nafion® density in images consistent with loading
- **35 wt.%** loading: Nafion® forming dense clumps with low infiltration into dense porous carbon
- **50 wt.%** and **60 wt.%**: Nafion® infiltrating porous carbon and forming thick films on surface
- **Highlight:** Lower activity observed with 35 wt.% Nafion® compared to higher loadings consistent with low Nafion® infiltration into dense porous carbon

Cathode and Fuel Cell Modeling

Microstructurally Consistent Model Framework



Multiphase model with separate water retention curves from pore diameter distributions for micropores and macropores in cathode

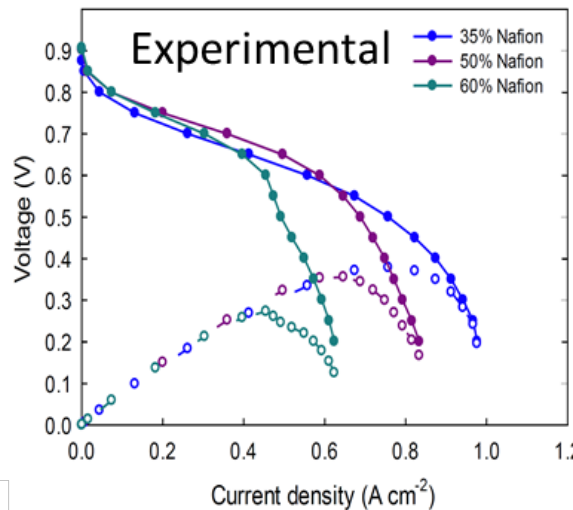
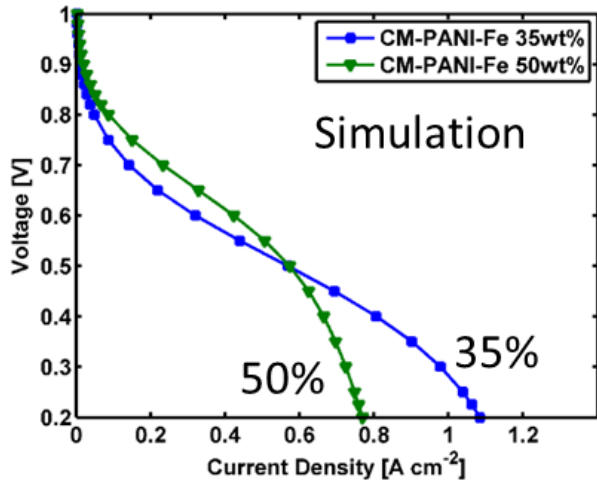


- Hydrophilic Nafion® coated
- Negative $p_{capillary}$: ($p_{cap} = p_l - p_g$)
 - Small pores filling first

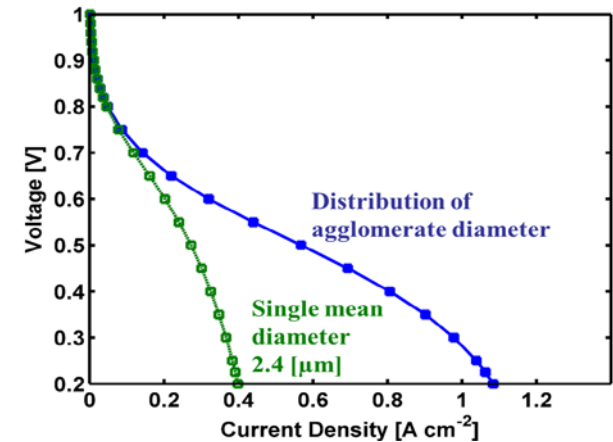
- Cathode model obtained using morphological property distribution inputs from nano-XRT imaging and transport property simulations
- Electrode model integrated into full cell model and validated against MEA testing

Fuel Cell Model Validation

Simulated and Experimental Fuel Cell Polarization Plots (H₂-Air Operation)

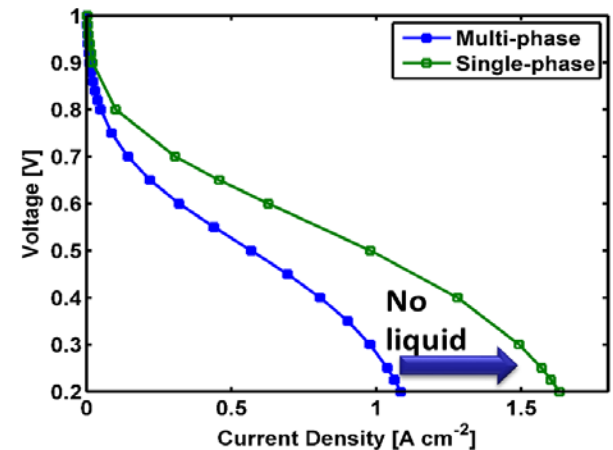


Effect of Agglomerate Size Distribution vs. Average Value



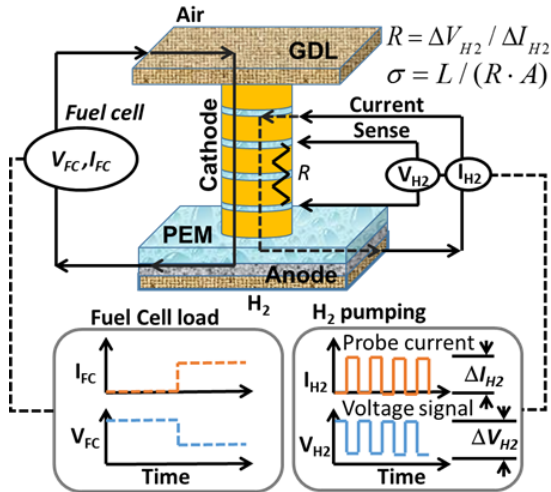
- **Highlight:** Model validated against experimental H₂-air fuel cell data with varying Nafion® loading
- Morphological parameters observed and calculated from nano-XRT – the only parameters modified in the model
- Carbon agglomerate size distribution having large impact on fuel cell performance prediction; single-diameter model insufficient
- **Highlight:** Hypothetical case of no-liquid water identifying path to significant performance improvement of non-PGM MEAs

Effect of Eliminating Liquid Water

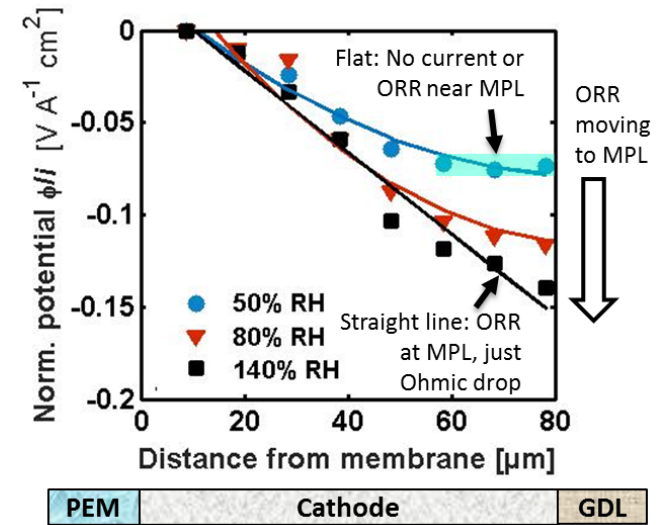
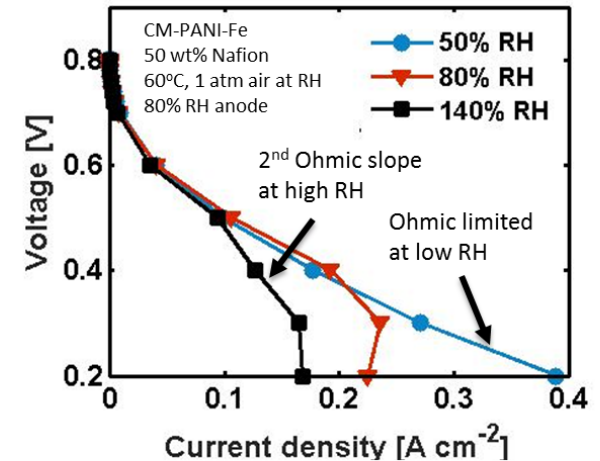
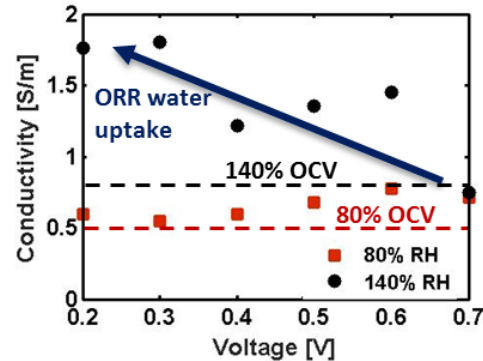


Microstructured Electrode Scaffold (MES): ORR and Conductivity

Anode: 0.2 mg cm⁻² Pt; **Cathode:** 5 cm², CM-PANI-Fe-C catalyst, 4.0 mg cm⁻²; 50, 80, 140 % RH
Cell testing: 60°C; 80% RH (anode and membrane), 1 atm air; **Membrane:** 212 Nafion®

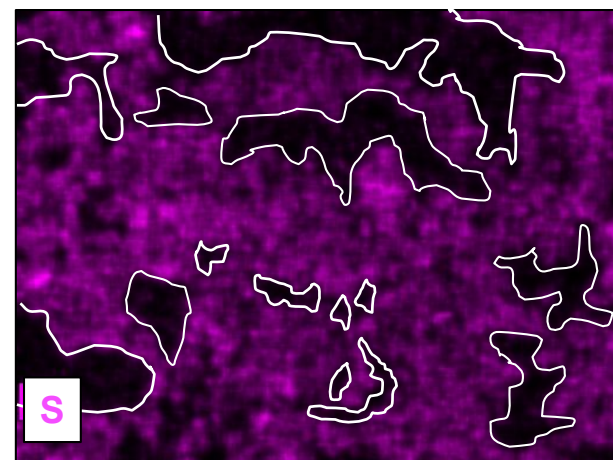
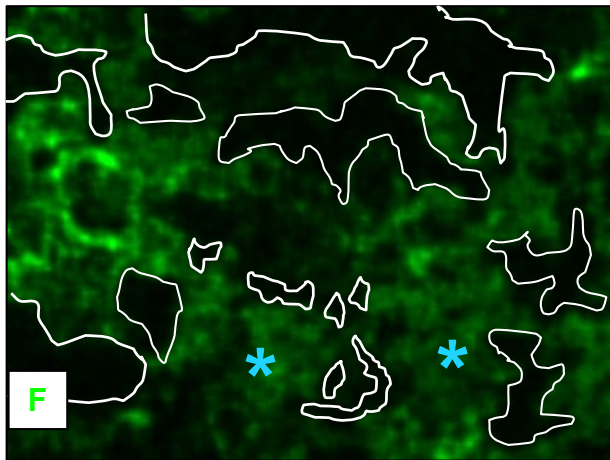
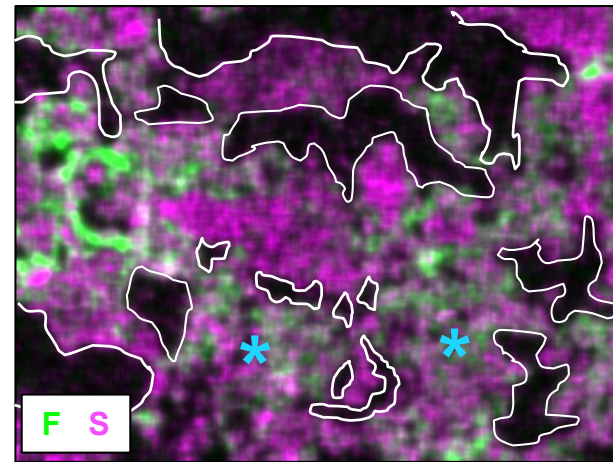
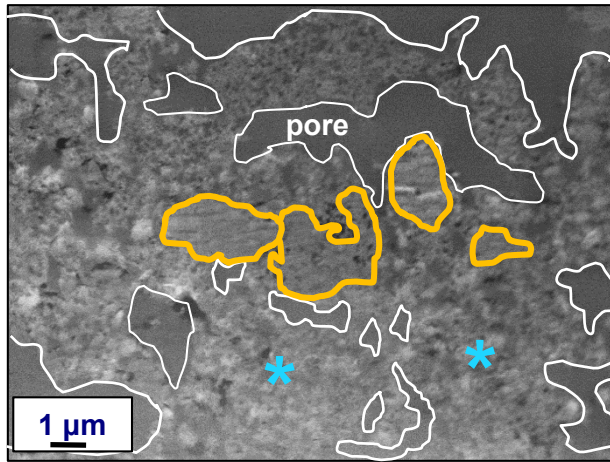


Direct conductivity measurement during PEFC operation on air



- Potential distribution in Nafion®: Slope proportional to local ORR rate
- **50% RH:** Limited proton transport; ORR occurring primarily near PEM, restricted near GDL (→ flat potential profile)
- **140% RH:** Large iR -drop due to water accumulation giving rise to second Ohmic slope (validation of the model); ORR occurring near the GDL; water production significantly increasing proton conductivity, even with >100% RH feed

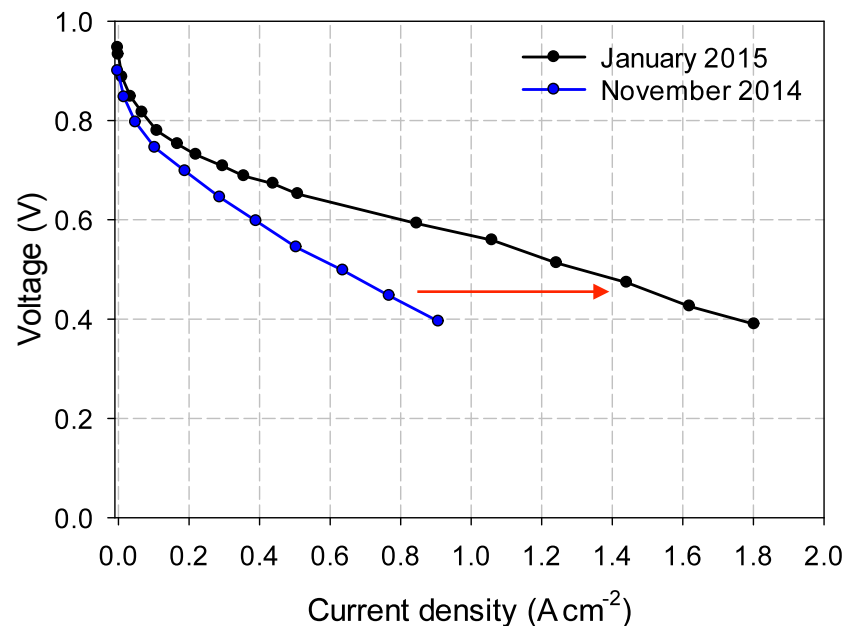
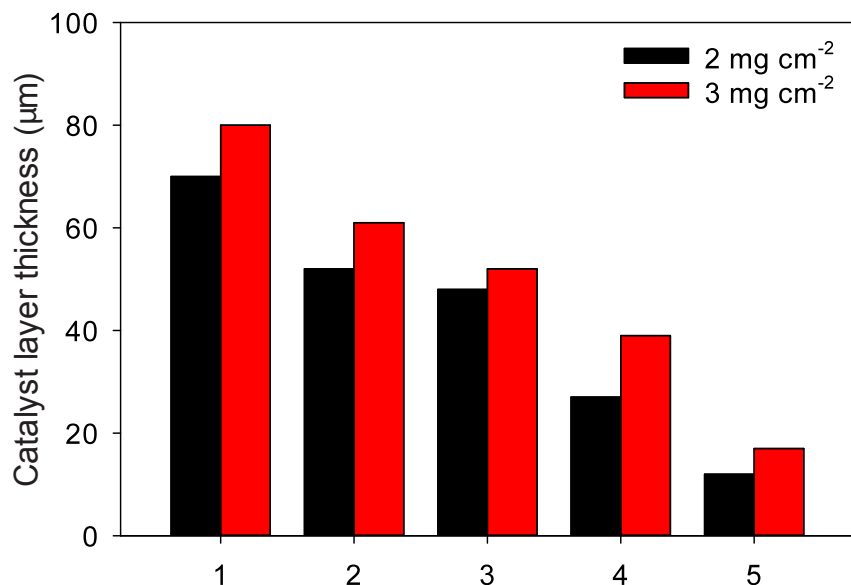
Elemental EDS Mapping from Region Near Membrane/Electrode Interface



- **Highlight:** Uniform distribution of ionomer (F, green) and catalyst associated with carbon-rich phase (S, pink) from the membrane and across the CM-PANI-Fe-C catalyst layer
- Ionomer impregnating fibrous part derived from CM + PANI (*) but not dense catalyst part (orange outline); morphological property of the catalyst layer

MEA Fabrication: Processing of Catalyst Layers with Varied Thicknesses

Anode: $0.2 \text{ mg}_{\text{Pt}} \text{ cm}^{-2}$ Pt/C H_2 , 200 sccm, 1.0 bar H_2 partial pressure; **Cathode:** ca. 4.0 mg cm^{-2} CM-PANI-Fe-C; O_2 , 200 sccm, 1.0 bar O_2 partial pressure; **Cell:** 80°C , 100% RH



- Electrodes manufactured with varied thickness while keeping loading and electrode composition intact
- **Highlight:** Modifications to the electrode structure resulting in much thinner catalyst layer and significantly improved fuel cell performance

Collaborations

- **Partners in this project: seven organizations with highly complementary skills and capabilities in catalyst development, electrode structure design, materials characterization, MEA fabrication, fuel cell system development and commercialization:**
 - ✓ Los Alamos National Laboratory (direct DOE-EERE contract)
 - ✓ Oak Ridge National Laboratory (direct DOE-EERE contract)
 - ✓ Carnegie Mellon University (subcontract to LANL)
 - ✓ University of Rochester (subcontract to LANL)
 - ✓ University of Waterloo (subcontract to LANL)
 - ✓ IRD Fuel Cells (subcontract to LANL)
 - ✓ General Motors (collaborative research and development agreement, CRADA, with LANL)
- **Collaboration with organizations not involved in this FCTO project:**
 - ✓ Strategic Analysis, Arlington, Virginia – non-PGM catalyst cost analysis
 - ✓ Northeastern University, Boston, Massachusetts – ORR mechanism
 - ✓ Stanford University, Palo Alto, California – soft X-ray studies
 - ✓ Fraunhofer Institute for Chemical Technology, Pfinztal, Germany – non-PGM catalyst corrosion
 - ✓ Argonne National Laboratory, Lemont, Illinois – hard X-ray studies; catalyst development
 - ✓ University of Chicago, Chicago, Illinois – hard X-ray studies (data processing and interpretation)
 - ✓ Pajarito Powder, Albuquerque, New Mexico – non-PGM catalyst scale-up and commercialization
 - ✓ Chevron Energy Technology Company, Richmond, California – CRADA on non-electrochemical application of non-PGM carbon-based materials

Remaining Challenges and Barriers

- Oxygen reduction reaction activity of non-PGM catalysts (required to lower cost of stack components)
- Long-term stability and performance durability of non-PGM catalysts
- Understanding of the active-site and reaction mechanism to allow bottom-up catalyst design
- Electrode integration for (i) sufficient ionic and electronic conductivity in thick catalytic layers and (ii) efficient mass transport to/from the active reaction sites
- Scale-up of non-PGM catalyst synthesis (beyond the already accomplished batch-size of *ca.* 100 g)
- Water management at high current densities
- Optimization of ionomer distribution in the electrode layer
- MEA design, optimization, fabrication, and scale-up
- Integration with existing automotive fuel cell stack and system technology

Summary

- June 2015 ORR selectivity and durability targets achieved and exceeded:
 - ✓ Potential loss of **~30 mV** at $E_{1/2}$ after 30,000 cycles between 0.2 and 1.0 V
 - ✓ H_2O_2 yield of less than **2%** across the entire potential range
- Fuel cell voltage of **0.86 V** reached at 0.044 A cm^{-2} with advanced CM-PANI-Fe-C catalyst (nearing 2020 DOE target of 0.87 V)
- Promising activity achieved with **Fe-free catalyst** (CM-PANI-Co-C) in RDE and fuel cell testing (with a relatively low loading)
- Combination of DFT modeling, NRVS, and $\Delta\mu$ -XAS studies pointing to the presence of surface active **Fe-N_x** sites; from DFT studies, multi-metal Fe_2N_5 sites found to be likely the key moiety, in agreement with NRVS- $\text{NO}_{(g)}$ probing
- Decrease in ORR activity linked to degradation of surface active sites; correlation of cell performance loss with XAS yielding another evidence for the existence of **Fe-N_x** active sites
- DFT studies of thermodynamic limiting potential, U_L , revealing the most active ORR structure to date: **FeCoN₅(OH)** ($U_L = 0.80 \text{ V}$ versus computational hydrogen electrode)
- Cs^+ -staining of Nafion[®] allowing for separate mapping of catalyst and Nafion[®] distribution at 50 nm resolution; **cathode model** developed from nano-XRT imaging and validated against experimental studies with different Nafion[®] loadings
- **All project performance measures** and **milestone** either met (some exceeded) or remaining on schedule

Catalyst Development:

- Completion of remaining activity/durability catalyst performance targets
- Enhancement of the ORR activity of Fe-free catalysts
- Further development of two-nitrogen precursor catalysts, focusing on activity and durability

Active Site and Durability Studies:

- *In situ* XAS studies in combination with DFT-FEFF calculations for active site determination
- Completion of the Mössbauer study of active sites using molecular probes
- Determination of corrosion rate measurements; comparison with Pt/C catalysts

Electrode Design and Modeling:

- Electrode structure and modeling analysis of scaled IRD and GM electrodes using nano-X-ray tomography (nano-XRT)
- Detailed modeling of microstructured electrode scaffold (MES) system for model improvement; parametric studies of electrode formulation by MES

MEA Optimization and Fabrication:

- Completion of electrode optimization study; optimization of the first-generation spray-coated MEAs; fabrication and testing of 50 cm² MEAs

Co-Authors



- **Catalyst research and characterization; project management**
Piotr Zelenay (Project Lead), Hoon Chung, Edward Holby, Ulises Martinez, Gerie Purdy, Urszula Tylus



- **Catalyst and electrode characterization**
Karren More (PI), David Cullen



- **Electrode characterization, modeling and design**
Shawn Litster (PI), Siddharth Komini Babu



UNIVERSITY OF
ROCHESTER

- **Catalyst characterization**
Michael Neidig (PI), Jeffery Kehl, Jared Kneebone



- **Catalyst development and characterization**
Zhongwei Chen (PI), Drew Higgins, Gaopeng Jiang, Min-Ho Seo



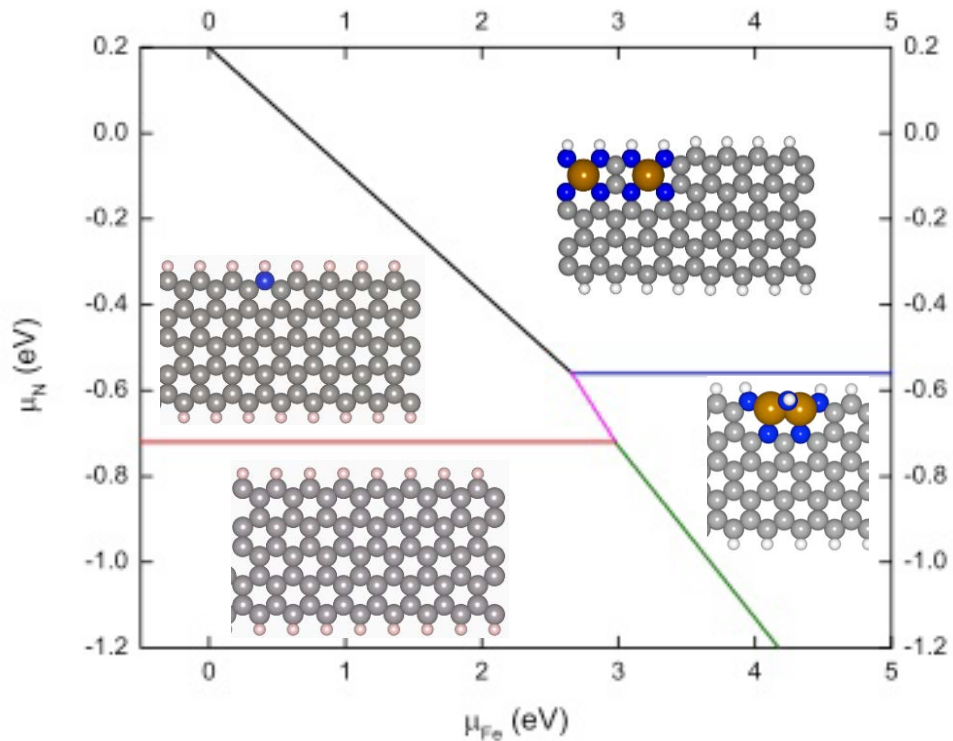
- **MEA design, integration, testing and scale-up**
Madeleine Odgaard (PI), Debbie Schlueter



- **Electrode and MEA research; MEA validation**
Joseph Ziegelbauer (PI)

Back-Up Slides

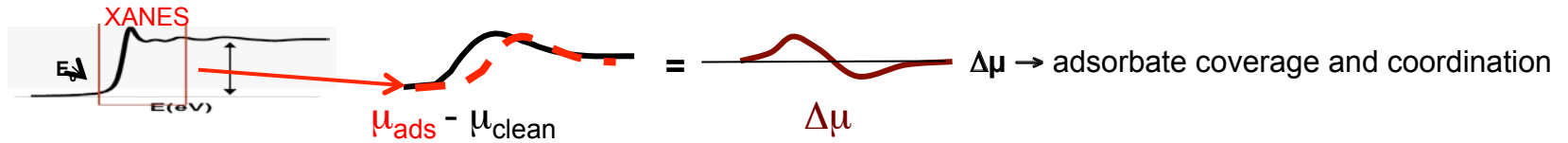
DFT-based Phase Diagram of Stable Active-Site Structures



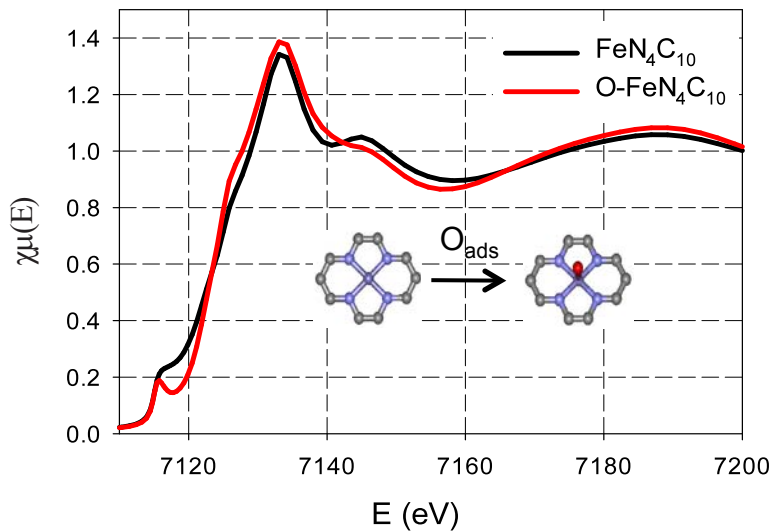
Monte Carlo study *via* semi-empirical potentials confirmed by DFT; three structural motifs:

- N coordinates Fe
- N-Fe complexes most stable at edge
- N-Fe edge complexes thermodynamically driven to form clusters

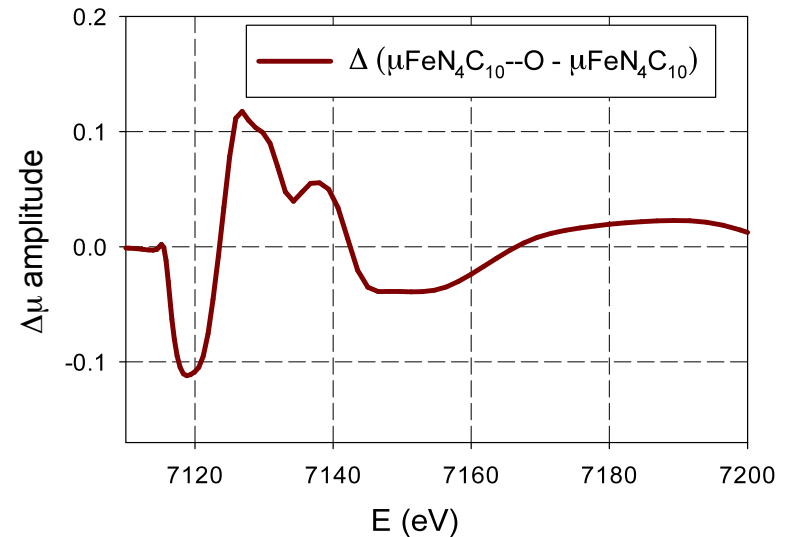
§#: Surface-Adsorbate Interactions as a Function of Applied Potential



FEFF calculation of theoretical spectra of Fe K-edge



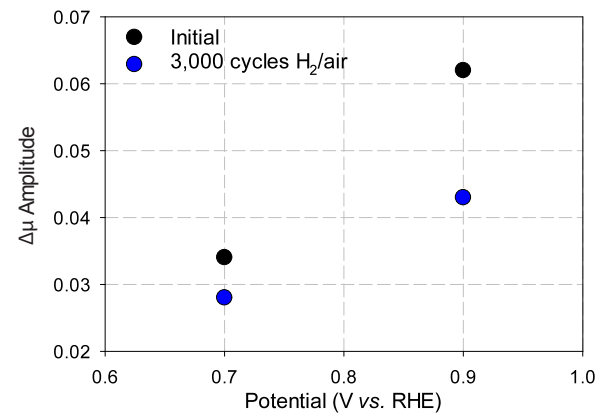
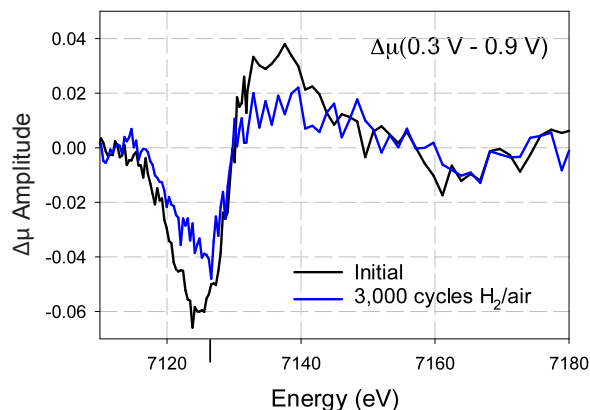
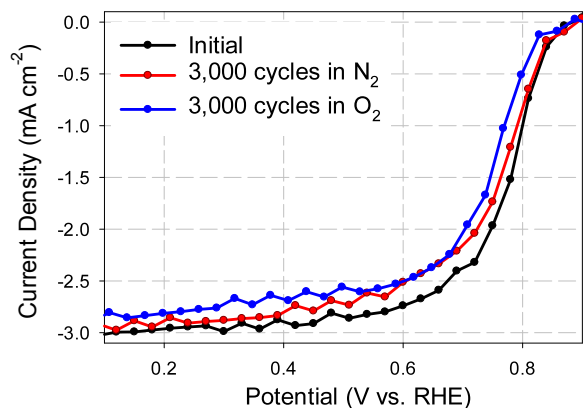
$\Delta\mu$ obtained by subtraction of theoretical Fe K-edge



- **FEFF:** Effective scattering of photoelectrons linking atomic-scale structures to §# signatures
- §# signal sensitive to type of species and Fe environment
- Peaks within 5 eV of experimental §# → good fit
- DFT structures with and without adsorbates serving as input to FEFF for comparison to §#

In situ XAS/XANES Study of Fe-CM-PANI Performance Degradation

RDE: 0.5 M H₂SO₄; 900 rpm; 25°C; Hg/HgSO₄ (O₂ sat. 0.5 M H₂SO₄) reference electrode; graphite counter electrode; steady-state potential program: OCP, 300 s, 30 mV steps, 30 s/step; **Cycling (RDE):** 3,000, 0.5 M H₂SO₄/O₂ and 0.5 M H₂SO₄/N₂; **XAS experiments:** 0.5 M H₂SO₄/air AgAgCl reference electrode, 5 cm² electrode; catalyst loading 4.0 mg cm⁻²; **Cycling:** 3k 0.5 M H₂SO₄/air

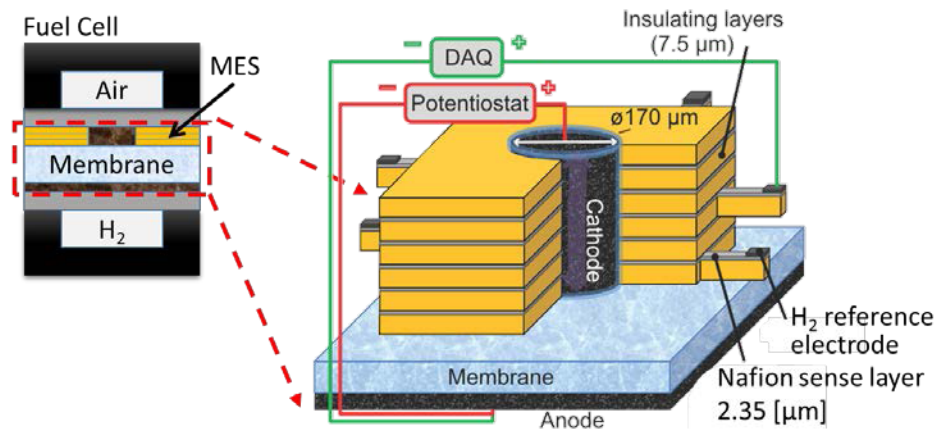


- Loss in performance after cycling in air → decrease of $\Delta\mu$ amplitude (indicative of Fe-N removal)
- **Fe-N moiety responsible for ORR activity**; developed method for observation of active site loss

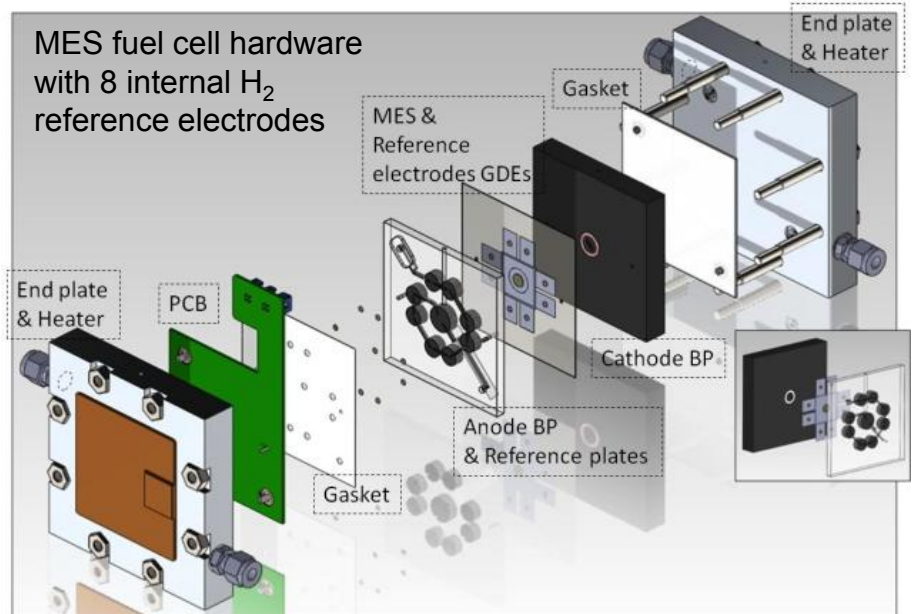
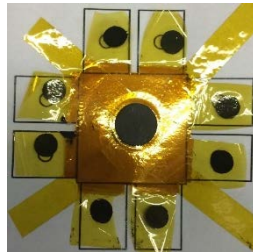
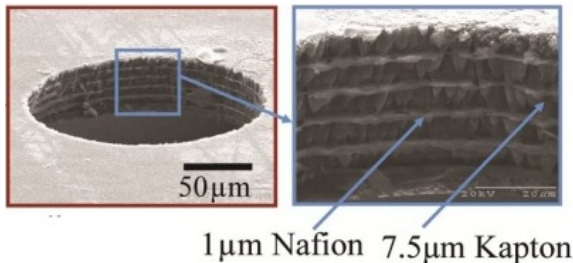
Reaction Distribution Measurements

- Microstructured electrode scaffold (MES) diagnostics for measuring distributions across the thickness of operating electrodes.
- Measurement of Nafion® potential through cathode thickness to observe ORR distribution through thickness and measure conductivity.
- Cylinder of cathode prepared in microfabricated cavity with Nafion® sense layers (electrolyte bridge) on the cavity perimeter spaced by Kapton® insulating layer. Integrated H₂ reference electrodes for potential measurement.
- 200 μm diameter and 87 μm deep cavity with potential measurements spaced by 10 μm.
- CM-PANI-Fe ink with 50 wt.% Nafion® loading inserted into cavity to form cathode.

MES for Measuring Nafion® Potential in Cathode



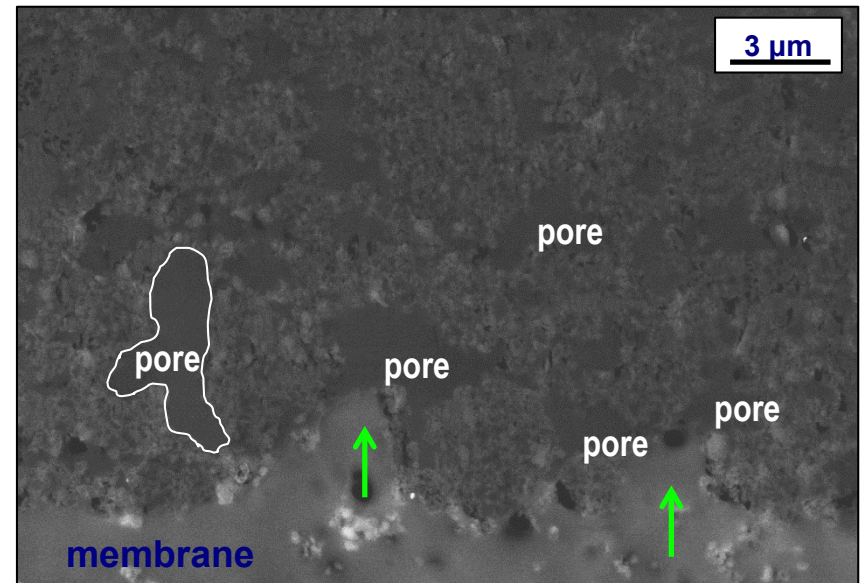
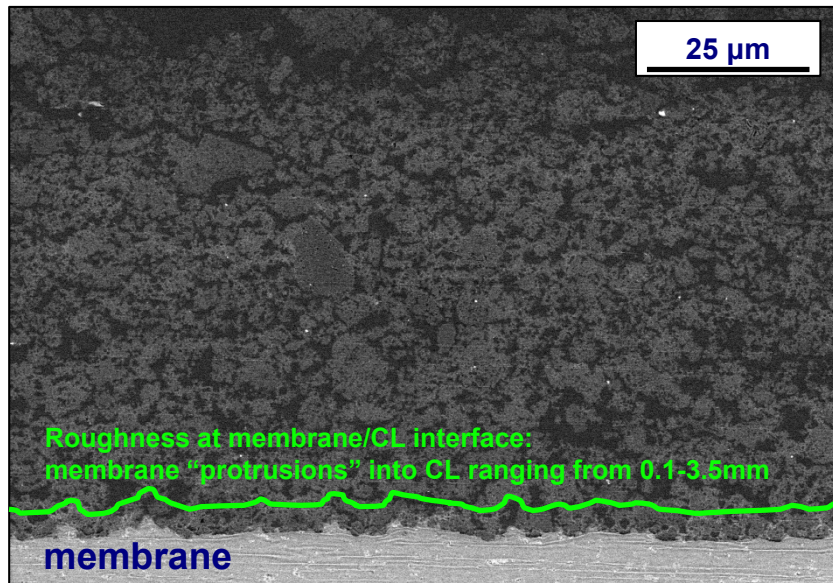
MES cavity with sense layers 8-layer MES



Hess, K. C., Epting, W., and Litster, S., *Analytical Chemistry*, 2011.

Microstructure and Chemistry of CM-PANI-Fe-C Catalyst Layer in MEA

Backscatter Electron (BSE) Image of Catalyst Layer (CL) Cross-section



- Uniform distribution of pores (dark regions) throughout catalyst layer (CL)
- BSE image showing rough membrane/CL interface – roughness ranging from 0.1 to 3.5 μm ; green line is offset replica of interface roughness
- Green arrows showing two membrane protrusions into the CL, directly associated with incomplete contact between membrane/CL interface